JAERI-Tech
2003-087

APPLICABILITY OF LBB CONCEPT TO TOKAMAK-TYPE FUSION MACHINE

December 2003

Masataka NAKAHIRA

日本原子力研究所
Japan Atomic Energy Research Institute

本レポートは，日本原子力研究所が不定期に公刊している研究報告書です。
入手の問合わせは，日本原子力研究所研究情報部研究情報課（〒319-1195 茨城県那珂郡東海村）あて，お申し越しください。なお，このほかに財団法人原子力弘済会資料センター（〒319-1195 茨城県那珂郡東海村日本原子力研究所内）で複写による実費頒布をおこなっております。

This report is issued irregularly.
Inquiries about availability of the reports should be addressed to Research Information Division, Department of Intellectual Resources, Japan Atomic Energy Research Institute, Tokai-mura, Naka-gun, Ibarakiken 319-1195, Japan.

編集兼発行　日本原子力研究所

Applicability of LBB Concept to Tokamak-type Fusion Machine

Masataka NAKAHIRA

Department of ITER Project
Naka Fusion Research Establishment
Japan Atomic Energy Research Institute
Naka-machi, Naka-gun, Ibaraki-ken

(Received October 22, 2003)

A tokamak-type fusion machine has been characterized as having inherent plasma shutdown safety. An extremely small leakage of impurities such as primary cooling water, i.e., less than 0.1 g/s, will cause a plasma disruption. This plasma disruption will induce electromagnetic forces (EM forces) acting in the Vacuum Vessel (VV) and plasma-facing components. The VV forms the physical barrier that encloses tritium and activated dust. If the VV has the possibility of sustaining an unstable fracture from a through crack caused by EM forces, the structural safety will be assured and the inherent safety will be demonstrated.

This paper analytically assures the Leak-Before-Break (LBB) concept as applied to the VV and is based on experimental leak rate data of a through crack having a very small opening. Based on the analysis, the critical crack length to terminate plasma is evaluated as about 2 mm. On the other hand, the critical crack length for unstable fracture is obtained as about 400 mm. It is therefore concluded that EM forces induced by small leak to terminate plasma will not cause the unstable fracture of VV, and then the inherent safety is demonstrated.

Keywords : *Fusion, ITER, Tokamak, Vacuum Vessel, Structural Safety, Crack Mouth Opening Displacement, Surface Tension, Leak, Molecular Flow, LBB*

トカマク型核融合装置におけるLBB概念の適用性評価

日本原子力研究所那珂研究所ITER開発室
中平　昌隆

（2003年10月22日受理）

トカマク型核融合装置は、プラズマの自動消滅という固有の安全性を有している。わずか0.1g/s以下の水リークによりプラズマが消滅するが、この際ディスラプションを起こすことがある。このプラズマディスラプションは、真空容器及びプラズマ対向機器に電磁力を発生させる。真空容器は、トリチウムや放射性ダスト等の物理障壁であり、もし貫通き裂からのリークによって発生する電磁力に対し、不安定破壊することがなければ、構造安全性は確保され、固有の安全性を実証することになる。

本報告では、上記の様な破断前漏洩(Leak Before Break, LBB)概念の真空容器への適用性を評価するため、解析モデルを構築し、クラック状の貫通き裂を模した真空リーク試験によりその妥当性を検証した。本解析により、プラズマを消滅されるための限界き裂長さは約2mmと見積もられ、一方真空容器を不安定破壊させる限界き裂長さは約400mmと見積もられた。従って真空容器は貫通き裂からのリークによって発生する電磁力に対し、不安定破壊することは無いと結論づけられ、構造安全性を確保するとともに固有の安全性を実証した。

那珂研究所：〒311-0193 茨城県那珂郡那珂町向山８０１－１

Contents

目　次

1. Introduction

A tokamak-type fusion machine is said to have inherent safety associated with plasma shutdown. The fusion reaction is self-bounded by physical limits on pressure or density. Plasma will therefore be terminated by the ingress of a small leak of cooling water from a through crack. The inherent plasma shutdown due to a small water leak can be a useful incident that assures structural safety. With regard to safety assurance, an essential principle is to assure the structural integrity of the physical barrier to enclose the radioactive materials and to prevent the undue release of radioactive materials. A requirement of structural integrity to a tokamak-type fusion machine such as ITER is unique. The barrier shall be designed to preclude through crack and to withstand electromagnetic forces (EM forces) caused by plasma disruptions triggered by plasma control error or others, as design conditions. The uniqueness is to include the EM forces caused by cooling water ingress from in-vessel components, because any inspection during service is not required in ITER owing to its difficulty. From a safety design aspect, even if the structural integrity is assured, we have to assume a defect or a crack for structural safety assurance.

A small water leak form through crack in the barrier may cause a plasma disruption although there is the other possibility to terminate plasma safely. The plasma disruption induces an EM force that acts in the barrier. This force caused by the leak acts only once, because the plasma terminates. If the barrier has a credible possibility to sustain an EM force without unstable fracture even when a through crack exists, the structural safety of the barrier will be assured and the inherent safety will be demonstrated. The approach to assure the structural safety with the above process is called as the Leak Before Break (LBB) concept in this paper.

We consider the ITER structure as a representative tokamak-type fusion machine. The physical barrier that encloses the radioactive materials is the plasma Vacuum Vessel (VV). The VV is a double-walled structure with pressurized cooling water between these walls [1]. The external VV wall surfaces are exposed to vacuum environments to control the release of impurities to the plasma on the inner side and to provide thermal insulation for the superconducting magnets on the outer side. The ITER VV is constructed from Type-316L stainless steeel, which has high ductility. This design makes it possible to detect leakage before the occurrence of a complete break of the VV by monitoring cooling water leakage or by direct termination of the plasma. Either occurrence precludes the escape of radioactive materials from the VV, because it still will be possible to maintain a vacuum in the VV.

In this paper, a systematic approach to assure the structural safety is developed. A new analytical model of through crack, leak and flow of cooling water is proposed, considering a local plastic behavior at crack tip for evaluating crack opening and a technique to evaluating undulation effects in the through crack, that have not been taken into account in the previous study. The results of the analytical model are verified in comparison with those of leak measurement using small test pieces with fatigue crack. The critical crack length in ITER VV to terminate plasma is analyzed using the proposed model. Finally assurance of structural safety of ITER VV is discussed, comparing the critical crack length to terminate plasma and critical crack length to cause unstable fracture of the VV.

2. Basic Considerations

2.1 Target Leak

The LBB concept has been applied to assure the structural safety of piping systems of light water reactors [2]. In this study, the LBB concept is used to examine a rupture, and a

leak rate in the order of 10 g/s, using two-phase critical flow models [3]. In the ITER in-vessel environment, a small water leak into the vacuum can be detected by monitoring increasing H_2O and O_2 partial pressures. The detectable partial pressure threshold is around 10^{-7} Pa using a mass spectrometer. Using an effective pumping flow rate of 200 m^3/s, a detectable leak rate must exceed $2x10^{-5}$ $Pa•m^3/s$, corresponding to around $1x10^{-8}$ g/s for H_2O.

Based on the plasma operational characteristics of ITER, a water leak larger than the above value is allowable. The main plasma parameters used this study are summarized in **Table 1** [2]. To estimate the allowable water leakage, the following conditions are assumed.

· The effect of O_2 dissociated from leaked water is as discussed below.

· The allowable limit is assumed a condition where the plasma switches from the H-mode to the L-mode.

· The L-mode power threshold P_{H-L} is assumed half of P_{L-H} [4], i.e., 25 MW.

· The amount of O_2 inputted to the plasma from the O_2 included in the leaked water is 10% [4].

· The impurity confinement time τ_{imp} is 5 times τ_E, i.e., 17 s.

· The amount of O_2 in the plasma is steady state (the leakage of O_2 into the VV is equal to the O_2 exhausted).

The impurity radiation from oxygen ions with a density that is 4% of hydrogen ion density is estimated to be 50% of the alpha heating power in the fusion plasma having an average ion temperature of 10 keV [5),6)]. This radiation is about 50 MW in the case of ITER. Thus, an increase of 1% O_2 impurity will cause a 12-MW radiation loss. The allowable limit condition is that a P_{LOSS} is less than the L-mode power threshold P_{H-L}. The P_{LOSS} is total particle power loss from plasma, which contributes to confinement of plasma by heating the scrape-off layer (SOL). This value is about 100 MW in ITER. Thus, if the P_{LOSS} is

reduced 75 MW to $P_{H\text{-}L}$ (25 MW) by impurity radiation, plasma will change to the L-mode. This power reduction is equal to 6% of O_2 impurity. In this case, the leak rate of O_2 (L_{O2}) into the VV is calculated as follows.

$$L_{O2} = \frac{n_i \cdot V_p \cdot 0.06 \times 16}{\tau_{imp} \cdot 0.1 \times 6.022 \times 10^{23}} \qquad (1)$$

$$= 0.078 \text{ g/s}$$

where,

n_i : average ion density

V_p : plasma volume

τ_{imp} : impurity confinement time

Thus, the allowable water leak is 0.088 g/s (0.078 x 18/16). Although the detectable leak rate is much smaller than this, we will discuss about the leak rate to terminate plasma, because large leak corresponds to large crack length which gives conservative estimation. This leak rate implies that a new flow model encompassing the molecular and viscous flow regions is required.

2.2 Through Crack, Leak and Flow Model

A model of a small-leak from through crack has been studied for application to the first wall of a fusion machine [7]. Here, we will address the occurrence of a small-leak problem under the condition that hot water leaks into the vacuum from a through crack in a plate under tension. A leak and flow model is presented in **Fig. 1**. For simplicity, the crack surfaces are assumed sufficiently smooth to assume laminar flow, and the temperature of the cooling water is assumed constant, even during phase changes. In the model, the pressure balance and mass flow continuity are considered at the water/vapor interface.

When the surface tension of water is large enough to balance the coolant pressure, water may evaporate in the crack. In this case, the pressure balance at the water/vapor interface is expressed as

$$P_l - P_S = S\left(\frac{1}{a} + \frac{1}{\delta}\right) \quad (2)$$

where,

P_l : water side pressure at water/vapor interface

P_S : saturation vapor pressure

S : surface tension of water

2a : crack length (see Fig. 2)

2δ : crack mouth-opening displacement (CMOD)

The mass flow continuity is expressed as

$$G_W(P_0, P_l, \mu_W, \lambda, \zeta) = G_V(P_s, P_b, \mu_V) \quad (3)$$

where,

G_W, G_V : mass flow rates of water and vapor, respectively

P_0 : pressure of cooling water

P_b : vacuum pressure

μ_W, μ_V : coefficients of viscosity of water and vapor, respectively

λ : hydraulic friction factor for water flow

ζ : pressure loss coefficient in water flow region

The mass flow rate of water is given by the equation of flow in the slit [8].

$$G_W = \rho \cdot Q_W \quad (4)$$

where,

$$Q_W = \frac{\Delta P_W}{S1} \qquad \text{for } L_W >> Le \quad (5a)$$

$$= \frac{-S1 + SS}{2 \cdot S2} \qquad \text{for others} \qquad (5b)$$

$$\Delta P_W = P_0 - P_1$$

$$S1 = \frac{12 L_W \cdot \mu_W}{A \cdot B^3}$$

$$S2 = \frac{\zeta \rho}{2 A_R^{\ 2}}$$

$$SS = \sqrt{S1^2 + 4 S2 \cdot \Delta P_W}$$

$$Le = 0.04 \circ B \circ Re$$

ρ : density of the cooling water

Q_W : volume flow rate of the water

L_W : flow length of water

Le : entrance length

A : crack-opening length approximated to rectangular slit

B : crack-opening displacement approximated to rectangular slit

A_R : crack-opening area (A∘B)

Re : Reynolds number

The mass flow rate of vapor is given as follows [9].

$$G_V = \frac{A_R \cdot C \cdot \Delta P_V}{T_V \cdot R} \qquad (6)$$

where,

$$C = \frac{A \cdot B^3 \cdot P_{av}}{12 L_V \cdot \mu_V} \qquad \text{for viscous flow} \qquad (7a)$$

$$= 36.4 \sqrt{\frac{T_V}{M}} \qquad \text{for molecular flow} \qquad (7b)$$

$\Delta P_V = P_S - P_b$

$P_{av} = \frac{P_S + P_b}{2}$

L_V : flow length of vapor

T_V : temperature of vapor

R : gas constant (461.5 J/kg•K for water)

M : molecular weight (18 g/mol for water)

Crack opening area A_R is directly related to the crack mouth opening displacement (CMOD) [10]. The crack profile considered in this paper is shown in **Fig. 2**. This simulates the existence of a small-penetration opening at the bottom of a grown crack. If the CMOD can be described by the crack length at any position in the wall thickness, the equations for the through with uniform length in the wall thickness are used. This assumption is verified later (See Chapter III). It can be expressed by elastic theory as follows [11].

$$2\delta_e(\xi) = \frac{4\sigma_{ap} \cdot a}{E}\sqrt{1-\xi^2} \qquad (8)$$

where,

$\xi = \frac{x}{a}$ $(0 \le x \le a)$

$2\delta_e(\xi)$: crack mouth-opening displacement (CMOD) at position x by elastic theory

σ_{ap} : applied tensile stress

E : Young's modulus

On the other hand, Goodier and Field obtained an equation of the CMOD expressed by plastic theory as follows [12].

$$2\delta_p(\xi) = \frac{2\sigma_y \cdot a}{\pi E}\sec\theta_2 \cdot \left[\cos\theta \cdot \ln\left(\left(\frac{\sin(\theta_2 - \theta)}{\sin(\theta_2 + \theta)}\right)^2\right) + \cos\theta_2 \cdot \ln\left(\left(\frac{\sin\theta_2 + \sin\theta}{\sin\theta_2 - \sin\theta}\right)^2\right)\right] \qquad (9)$$

where,

$$\theta_2 = \frac{\pi\sigma_{ap}}{2\sigma_y}$$

$\theta = \cos^{-1}(\xi \cos\theta_2)$

$2\delta_p(\xi)$: CMOD at position x expressed by plastic theory

σ_y : yielding stress

Thus, a residual CMOD is given as follows.

$$2\delta = 2\delta_p(0) - 2\delta_e(0) \tag{10}$$

The evaporation rate m [kg/m^2 s] of cooling water in a large space is given by [9)]

$$m = 4.37\times10^{-3}\, P_S \sqrt{\frac{M}{T_V}} \tag{11}$$

In the present flow model, two leakage patterns can be considered. When the CMOD is small and when the water/vapor interface appears in the crack, a vapor leak will occur. In this case, its leak rate may not exceed the value given by Eq. (11), because the evaporation occurs in a closed space. The pressure balance and mass flow continuity determine the location of the water/vapor interface. When the CMOD is large, ingress of water will occur.

Although Eq. (3) is nonlinear, it can be solved by a simple iteration method. Therefore, the set of Eqs. (2) and (3) enables the examination of the leak rate as a function of operation temperature and pressure, applied stress, crack size, and plate thickness.

2.3 Geometrical Model of Leak Path in Through Crack

A fatigue crack with an undulating surface is a realistic leak path. The undulation along the leak path should be considered when evaluating the effective path length, the effective opening displacement, and pressure loss factor due to elbows. Narabayashi et al.

established a new pressure loss model for flow in a fatigue crack using measured surface roughness and undulation [13]. They obtained the undulation curve by fitting the measured surface roughness profile of an experimental fatigue crack. Following this technique, the undulation curves of a crack on test piece 43 (described below) as a typical example is obtained, as shown in **Fig. 3**. The major parameters of this profile are summarized in **Table 2**. The leak path shown in **Fig. 4** can be visualized from the measured profile of surface roughness and the calculated CMOD of the front and back surface using Eq. (10) (the values of the CMOD are shown in Table 4). A linear distribution of the opening displacement along the plate thickness is assumed.

It is easily understood from Fig. 4 that the crack opening width is calculated by,

$$2\delta^* = \psi \cdot 2\delta \qquad (12)$$

where,

$2\delta^*$: effective CMOD in the crack

ψ : the direction cosine of the crack profile

2δ : CMOD defined by Eq. (9) or (10)

The minimum direction cosine of the crack profile defines the minimum crack opening. This minimum crack opening should be used for evaluating the leak rate, because the surface tension becomes maximum, which is critical for the pressure balance. The R_{max} and undulation pitch are used to define the elbows in the crack for obtaining the pressure loss coefficient ζ_{elbow} as follows.

$$\zeta_{elbow} = N_{elbow} \cdot (0.946 \cdot \sin^2 \theta_{elbow} + 2.05 \cdot \sin^4 \theta_{elbow}) \quad [8] \qquad (13)$$

where,

$N_{elbow} = \dfrac{t}{L_\lambda \cos\theta_{elbow}}$: number of elbows in the crack

$\theta_{elbow} = \arctan\left(\frac{2R_{max}}{L_\lambda}\right)$: angle of the elbow

t : thickness of the wall

L_λ : undulation pitch

R_{max} : maximum height of irregularities

2.4 Critical Crack Length for Unstable Fracture in ITER VV

The electromagnetic loads acting on the VV are nonuniform in the poloidal direction, resulting in local damage instead of damage to the entire structure. A 3D FEM stress analysis has been performed using a 1/40 toroidal sector of the ITER VV postulating the electromagnetic (EM) load during disruption [14]. The analysis model and loading conditions are shown in **Fig. 5**. The blanket and the divertor in this figure are in-vessel components [15]. **Figure 6** shows that a maximum membrane stress of 138 MPa appears as a tensile stress at the corner of the lower port connection. Therefore, the extension of a crack is possible due to the disruption load. For simplification, it is assumed that the crack is initiated at the maximum stress point P1 and propagates along the assessment line shown in Fig. 6. The effect of the rib to restrain the crack propagation is neglected. Only the opening mode is considered since the membrane stress is dominant, and the effect of bending stress is not taken into account. The stress concentration factor at the tip of the crack has been estimated as shown in **Fig. 7**, with a crack length normalized by width to the adjacent port, 1.77 m (See Fig. 6). The critical stress concentration factor, as a conservative condition, is set to 150 $MPa \cdot m^{0.5}$, less than half the fracture toughness. For the criteria to consider rapid crack propagation when the stress concentration factor reaches a critical value, the critical crack length for structural instability is more than 400 mm (distance from edge x/width ~0.22),

which would cause large water leakage. The LBB concept will help to maintain the structural safety of the VV when the crack size causing the plasma-termination water leak is less than the critical crack length of 400 mm.

3. Verification of the Calculation Model

To verify the amount of water leakage through the crack penetration to the vacuum, water leakage has been measured as a function of crack size ranging from 1 to 7 mm. The test pieces were Type-316L stainless steel with a width of 50 mm and thicknesses of 2 and 4 mm. Cracks were artificially formed in the test pieces by force controlled cyclic loads with stress ratios of 0.05. Crack penetration was detected by monitoring air leakage during the fatigue process. The area around the crack penetration was machined to the shape of disk with a 40-mm diameter. An initial notch using Electric Discharge Machining (EDM) to a depth of 1 mm was removed from the front (waterside) of the crack during this phase. **Figure 8** shows a test piece used for this experiment. The test piece was installed inside the vacuum chamber and subjected to pressures up to 0.3 MPa by water. Water leakage through the crack was measured by a quadrupole mass spectrometer connected to the vacuum chamber. **Figure 9** shows an overview of the test setup. The main specifications of these test devices are summarized in **Table 3**.

Table 4 summarizes the main parameters of the test pieces and the leak rate results. Crack lengths on the front and back correspond to those on the waterside and the vacuum-side of test piece surfaces, respectively. **Figure 10** shows an example of the data obtained, plotted with the time history of the measured pressure in the vacuum chamber. The pressure sharply rises and falls significantly after water input and then continues to monotonously decrease. The sharp pressure rise immediately after water input is considered to result from

a leak of the vapor or air filled test piece holder before water input. The test piece holder was evacuated previously but small vapor or air remained. This is inherent in test systems and will not occur in an actual situation, because the double wall is filled with water before crack penetration. Thus, the leak rates listed in Table 4 are calculated with the value 200 s after water input to avoid this test related phenomenon using the following equation.

$$Q = Ve \cdot \frac{dP}{dt} + Se \cdot P \qquad (14)$$

where,

Q : leak rate of water or vapor

Ve : effective test chamber volume

P : test chamber pressure

Se : effective water pumping speed

The results have shown the monotonous decrease of the leak, though steady state leak has been expected. It can be considered that the precipitated sediments in the crack reduced the opening. A Scanning Electron (SE) image of the crack area after the leak test is shown in **Fig. 11**. Small sediments have precipitated in the crack. It can be considered that the precipitated sediments in the crack reduced the opening. Thus, a monotonous reduction in the leak rate was observed. The Electron Probe Micro Analysis (EPMA) of the sediments shows that they contained Al, Ti, Pb, and O. These elements are contained in the lubricants or working oil of valves or the vacuum pump. On the other hand, the freezing of water due to latent heat removal as a result of evaporation also should be considered as a cause of the opening reduction. The latent heat removed by evaporation q_{lh} at freezing temperature (273 K) is as follows.

$$q_{lh} = 2.44 \cdot m$$
$$= 1.7\ [MW/m^2] \qquad (15)$$

The heat flow from the environment (300 K for the test condition) q_h is calculated as follows.

$$q_h = \frac{\lambda_h \cdot \Delta T}{\delta^*} \tag{16}$$

where,

λ_h : thermal conductivity of water

If $q_{lh} > q_h$, the water will freeze. For this, the δ^* is required to be larger than 9.7 μm. However, this is too large to keep the water/vapor interface in the crack, and water flows directly into the vacuum area. In this case, the volume expansion will cause water freezing in the chamber by the Joule effect, but this will not cause the reduction of the opening area. Considering the Joule-Thomson effect in the crack, the order of the coefficient is 10^{-7} [K/Pa]. Thus, it can be concluded that the freezing of water has not occurred in this test. In this very simple consideration, the limited thermal conductivity of the test piece, holder, and chamber and the effect of radiation heating from the baked chamber are not taken into account. Considering the operating condition of ITER, the cooling water temperature would be 473 K, and the inner shell is directly wetted by the water. In addition, radiation from plasma or in-vessel components would be much higher than in this test. Thus, the freezing of water due to vaporization would have a very low probability of occurring. Although further study is required to clarify these effects, they are too complicated to simulate. To simplify the opening reduction problem, we will therefore use a fitting parameter for these experiments.

For CMOD calculation verification, the measured and analyzed values are compared in **Fig. 12**. The residual CMODs calculated using Eq. (10) by Goodier are plotted with the measured values listed in Table 4. Test piece numbers and crack locations (front or back) are indicated for plotting measured values. Using Rice's equation [16], Eq. (17), calculated values are also shown in Fig. 12 for reference.

$$2\delta_R = \frac{\pi a \sigma_{ap}^{\ 2}}{2E\sigma_y} \qquad (17)$$

The results show that Goodier's equation correlates with the measured data, and thus this is chosen for the following analysis.

We will use ψ of Eq. (12) for the fitting parameter of the opening reduction. From the results shown in Fig. 12, test pieces 28 and 43 were selected for the fitting, because they have the minimum error for calculating the CMOD. **Figure 13** shows the relation of calculated leak rate and the varied fitting parameter ψ. Experimental results are shown as the short horizontal bars in this figure. A parameter of 0.25 to 0.3 for ψ provides good fits to the test results, so ψ = 0.27 was used in the calculation.

4. Assurance of Structural Safety by LBB Concept

Using the model described above, the leak rate of a through crack of the ITER VV has been estimated. The conditions for the calculation are shown in **Table 5**. It is well known that the propagation length of a surface crack is limited to three times the plate thickness when the plate is under tensional stress [17]. Thus, the half-crack length of the waterside was selected as 90 mm (60 mm x 3 / 2), the half length of the penetrated crack (plasma side), a^*, was varied. The analysis results show that the leak rate will exceed 0.088 g/s at the half length of the penetrated crack around 1 mm, as shown in **Fig. 14**, and also that this leak rate will terminate plasma. Thus, the critical crack length (full length of the crack) for plasma termination is estimated as about 2 mm. Even with this crack length, the rapid extension of the crack progressing to structural fracture of the VV is not expected. The result suggests that the through crack will immediately terminate plasma. This means that any through will not allow plasma operation. Considering the critical structural crack length of 400 mm, it

can be said that the plasma operation requirement is much more severe than the safety requirement.

5. Conclusion

A tokamak-type fusion machine is said to have inherent safety associated with plasma shutdown. Plasma will be terminated by the ingress of a small leak of cooling water from a through crack. In addition, ITER vacuum vessel, a barrier to the tritium and radioactive dusts, has high ductility of its material. Based on these promising characteristics, structural safety of the vacuum vessel has been assessed by clarification of critical crack lengths for plasma termination and for unstable fracture. The critical water leak rate to terminate plasma is evaluated as 0.088 g/s. To evaluate the critical crack length causing such small leak rate from a through crack, a new model has been proposed considering the plastic behavior of crack tip to evaluate crack mouth opening and the effect of undulated geometry of leak path. The model has been verified with measured results of leak rate using test pieces having fatigue cracks 1 to 7 mm in length. Using the model, the critical crack length to terminate plasma is evaluated as 2-mm in length. On the other hand, the critical crack length to cause unstable fracture of ITER vacuum vessel is assessed about 400 mm. The results show that a critical crack length to terminate plasma is monumentally less than the critical crack length to cause unstable fracture of the barrier. It can therefore be concluded that even when through crack exists, water leak will terminate plasma and the ITER vacuum vessel will sustain an electromagnetic force induced by plasma disruption without entire break. Thus, the structural safety of the ITER vacuum vessel can be assured, and therefore the inherent safety associated with plasma shutdown is demonstrated. The proposal on analytical model for evaluating a through crack and leak rate of cooling water and the assessment procedure

will be useful for assurance of structural safety of vacuum vessel. The author would like to propose to include such an attractive characteristic of plasma termination by a small leak not to cause unstable fracture as LBB concept, which was defined as leak detection and an affordable reactor shutdown before unstable break of pipes in the past.

Acknowledgements

The author would like to acknowledge Dr. E. Tada, Mr. K. Hada, Dr. Y. Neyatani, and Dr. Shibanuma of the Japan Atomic Energy Research Institute for their continuous suggestions and encouragement.

The author also would like to acknowledge the contributions of Dr. M. Shibui, Mr. Y. Yanagi, and Dr. N. Suzuki of the Toshiba Corporation, and Mr. H. Takahashi of the Hitachi, Co. Ltd. for their experimental and analytical support.

References

1) ITER Technical Basis, ITER EDA Documentation Series No. 24, IAEA, Vienna, 2002.
2) K.Shibata, et al., Overview of Reliability Test Program on Primary Coolant Piping of Light Water Reactors, J.Atom.Enrg.Soc.of Japan,35,10 (1993) 923-939.
3) F.J.Moody, Maximum Two-Phase Vessel Blowdown from Pipes, Trans. ASME, J.Heat Transfer (1966) 285.
4) N.A.Uckan, et al., ITER Physics-safety Interface : Models and Assessment, Fusion Technology, 30 (1996) 551-557
5) H.Ikegami, et al., Kakuyuugou kenkyuu I, The University of Nagoya Press, Aichi, 1996, pp. 25 [in Japanese].
6) D.E..Post, et al., Atomic Data and Nuclear Data Tables 20, 5 (1977).

7) M. Shibui, et al., Fail-Safe First Wall for Preclusion of Little Leakage, JAERI-M, 94-074 (1994)

8) JSME Mechanical Engineer's Handbook, (1987) A5-40.

9) H.Kumagai, et al.,Vacuum Science and Engineering, Syokabo, Tokyo(1970) [in Japanese].

10) M.D.German and V.Kumar, ASME, Jounal of Pressure Vessel Technology, Vol.105(1983)290-298.

11) E. Smith, Leakage through an Irregular Crack in a Pressurized Component, Int. J. Pres. Ves. & Piping 38 (1989) 333-339.

12) J.N.Goodier and F.A.Field, Plastic Energy Dissipation in Crack Propagation, Metallugical Soc. Confs., 20 (1962) 103-118.

13) T.Narabayashi, et al., Experimental study on leak flow model through fatigue crack in pipe, Nucl. Engng. Des. 128(1991)17

14) Y.Neyatani, et al., Study of decay heat removal and structural assurance by LBB concept of tokamak components, Proc. 18th IAEA Fusion Energy Conf., Sorrento, Italy, IAEA-CN-77/SEP/01 (2000).

15) ITER Final Design Report Cost Review and Safety Analysis, ITER EDA Documentation Series No. 14, IAEA, Vienna, 1999.

16) J.R.Rice, Journal of Applied Mechanics, Transactions, American Society of Mechanical Engineers, Vol.35, Series E, (1968),379-386

17) G.Yagawa, Fracture Mechanics, Baifukan, Tokyo(1988) [in Japanese].

Table 1 Main plasma parameters in ITER for allowable leak study

Parameters	Symbol	Value
Fusion power	P_{FUS}	500 MW
Alpha heating power	P_{α}	~100 MW
Loss power flow into the scrape-off layer	P_{LOSS}	~100 MW
H-mode power threshold	P_{L-H}	~50MW
Average ion density	n_i	$\sim 10^{20}$ /m^3
Plasma volume	V_p	831 m^3
Energy confinement time	τ_E	3.4 s

Table 2 Main parameters of leak path (TP43)

Parameters	Value
Maximum height of irregularities R_{max}	15.0 μm
Center line average height R_a	2.2 μm
Undulation pitch L_λ	0.37 mm
Max. direction cosine	1.00
Min. direction cosine	0.71
Average direction cosine	0.97

Table 3 Main parameters of test device

Parameters	Value
Volume of Chamber	3.94×10^{-2} m^3
Volume of Holder	3.77×10^{-4} m^3
Volume of Vacuum	3.91×10^{-2} m^3
Surface area of Vacuum	0.884 m^2
Pumping speed of TMP	0.3 m^3/s
Effective pumping speed for N_2	0.09 m^3/s
Effective pumping speed for H_2O	0.105 m^3/s

Table 4 Main Parameters of test pieces and results of the leak rate

Test Piece	Thickness t [mm]	Width W [mm]	Stress σ_{ap} [MPa]	Front 2a [mm]	Back 2a* [mm]		CMOD (front) [μm]	CMOD (back) [mm]
23	2.17	50.10	162.4	4.60	2.65	Measured	3.57	0.70
						Analyzed	0.95	0.54
26	1.91	50.01	239.2	2.33	0.78	Measured	-	0.26
						Analyzed	2.02	0.68
28	1.91	50.00	239.3	4.14	1.90	Measured	-	1.54
						Analyzed	3.59	1.65
41	3.89	50.05	205.1	4.30	3.15	Measured	2.03	1.17
						Analyzed	2.02	1.48
43	3.86	50.06	206.6	6.73	3.41	Measured	-	1.56
						Analyzed	3.25	1.65

Note) Thickness and width are measured data during crack propagation process

Test Piece	Test No.	Wall temp [°C]	Water pressure [MPa]	Vacuum pressure [Pa]	Leak rate [g/s]
23	23-2	150	0.20	1.48×10^{-2}	1.2×10^{-5}
26	26-1	150	0.28	1.21×10^{-3}	9.1×10^{-7}
	26-2	150	0.36	1.06×10^{-3}	7.9×10^{-7}
28	28-3	150	0.36	2.46×10^{-2}	2.1×10^{-5}
	28-7	150	0.33	9.68×10^{-4}	7.3×10^{-7}
41	41-1	150	0.98	2.00×10^{-5}	1.5×10^{-8}
43	43-1	150	0.20	1.88×10^{-4}	1.5×10^{-7}

Table 5 Parameters for assessment of water leak on ITER Vacuum Vessel

Parameters	Value
Water temperature	373 K
Water pressure	1.1 MPa
Vacuum pressure	1.0×10^{-5} Pa
Young's modulus	186 GPa
Yielding stress	234 MPa
Applied stress	100 MPa
Fitting parameter	0.27
Half length of the crack at front (water) side	90 mm
Half length of the crack at back (vacuum) side	Parameter (a*)

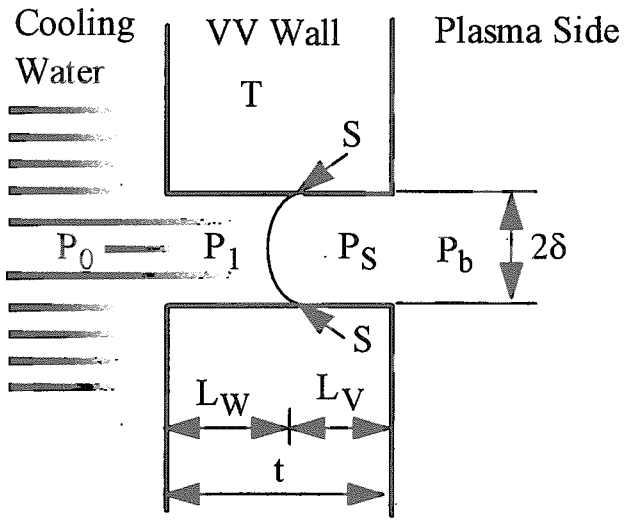

Fig.1 Flow model for small leak through crack

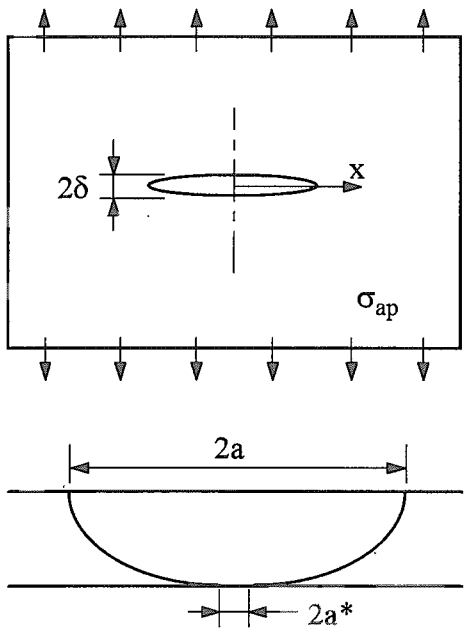

Fig. 2 Crack profile

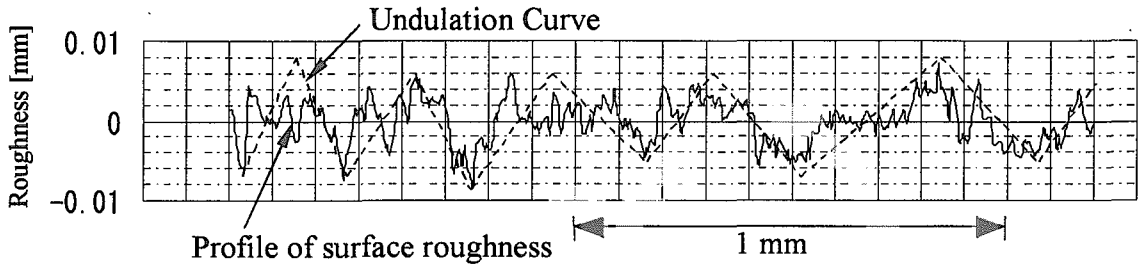

Fig.3 Undulation curve of a crack on test piece 43

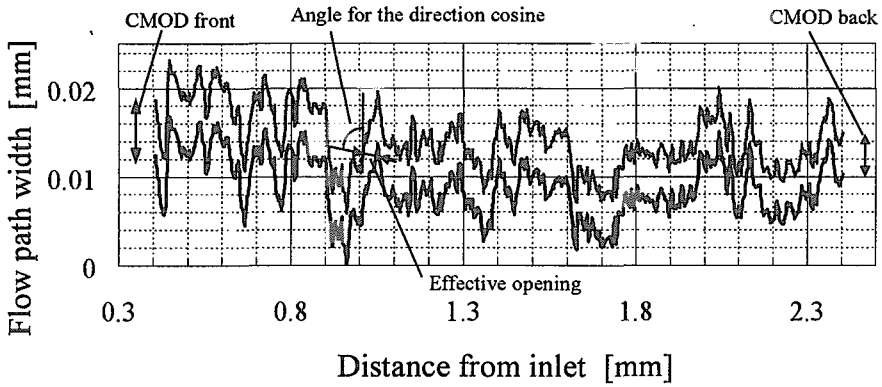

Fig.4 Leak path of a crack on test piece 43

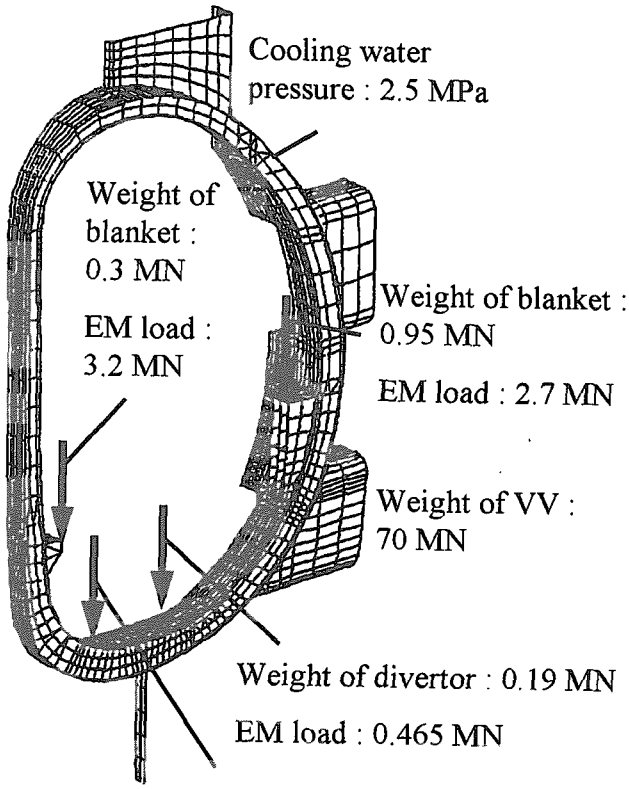

Performed for 1998 FDR model (1/40 sector)

Fig.5 Analysis model and loading conditions of ITER VV

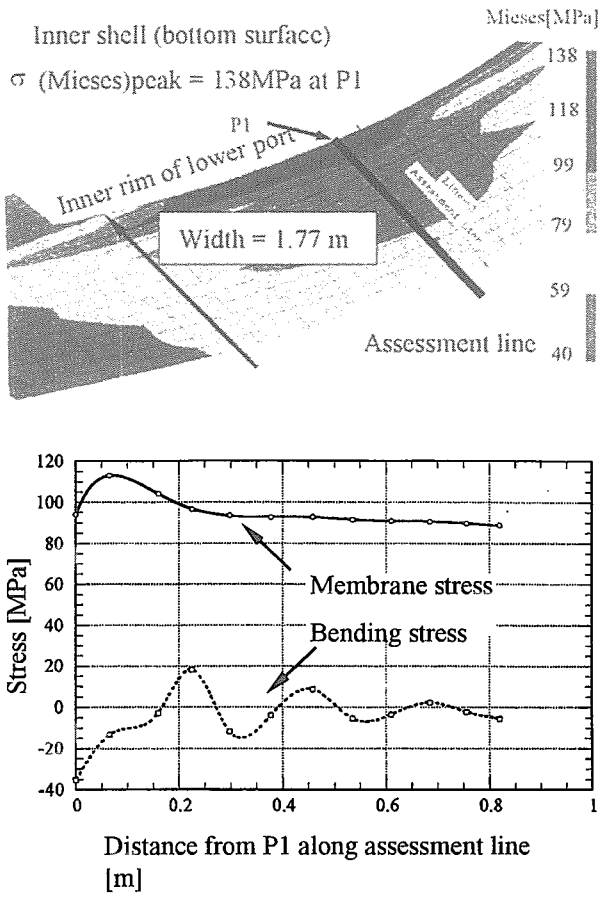

Fig.6 Location of the maximum membrane stress and assessment line

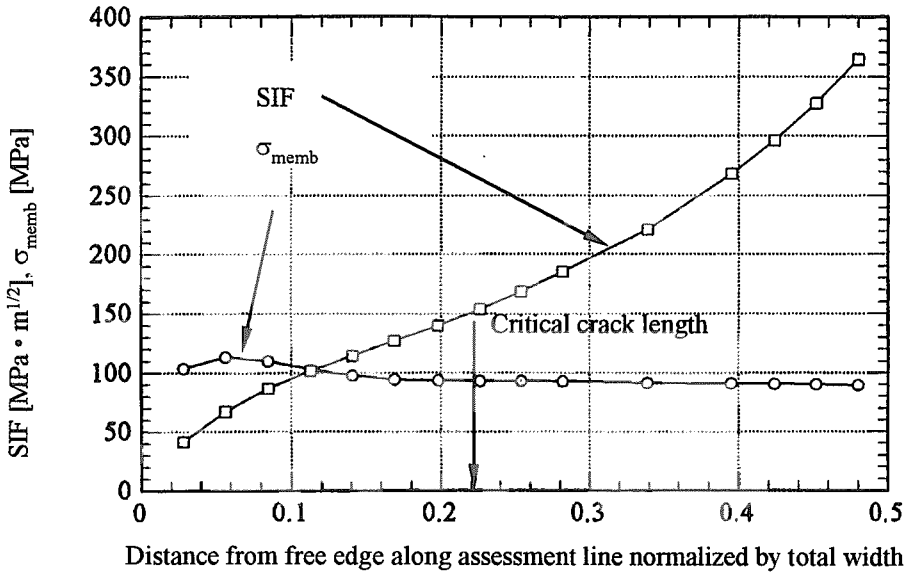

Fig.7 Estimated stress concentration factor at the tip of the crack along the assessment line

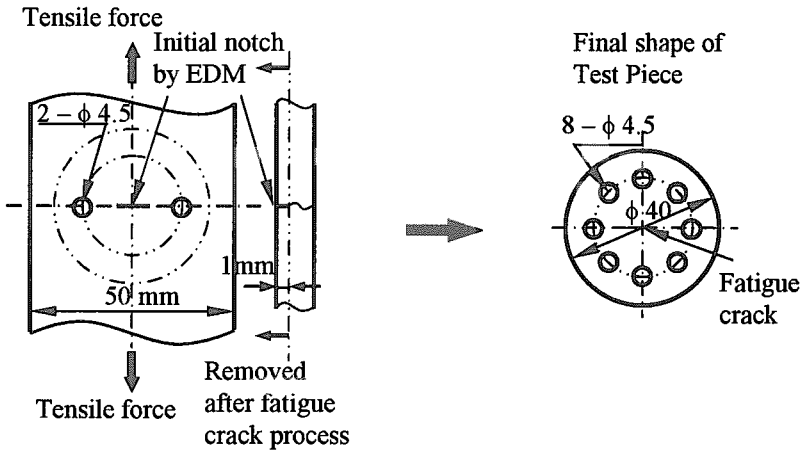

Fig.8 Test piece for water leak in vacuum environment

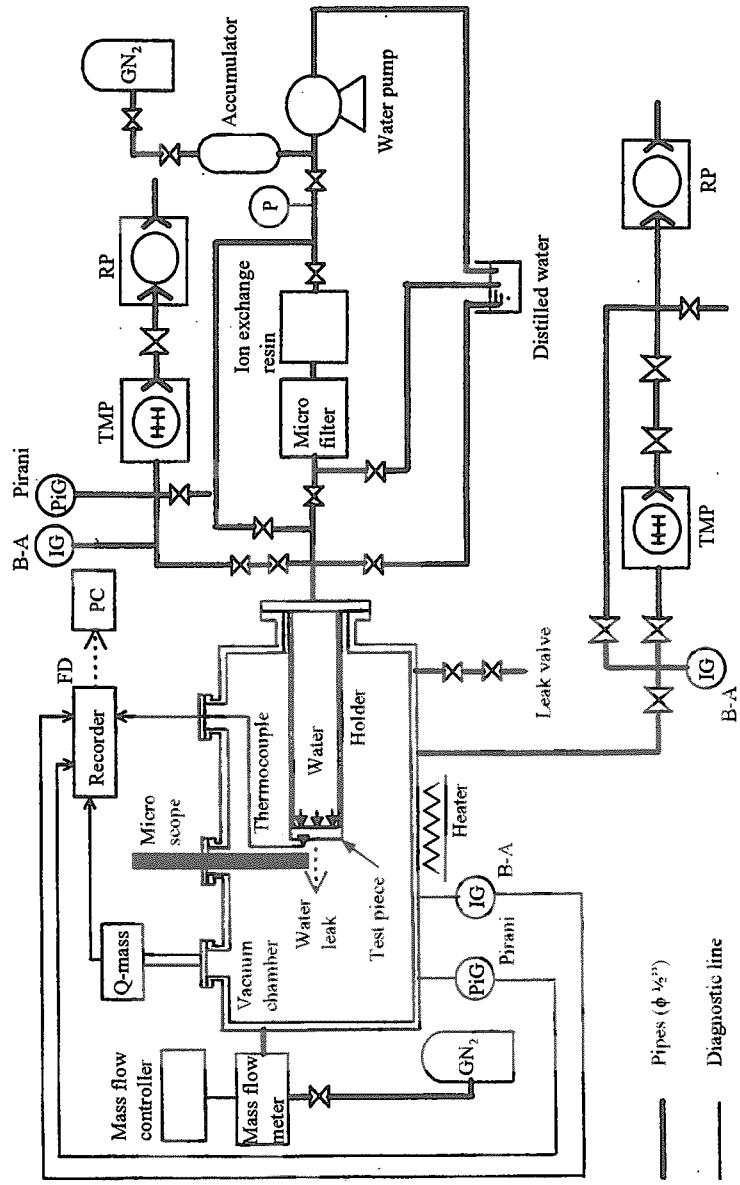

Fig.9 Overview of test devices for water leak in vacuum environment

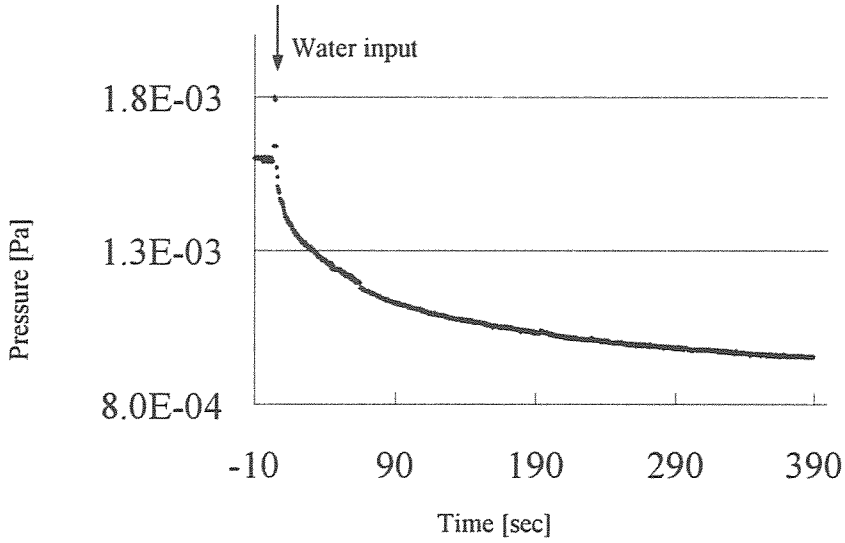

Fig.10 An example of obtained measured pressure (TP26)

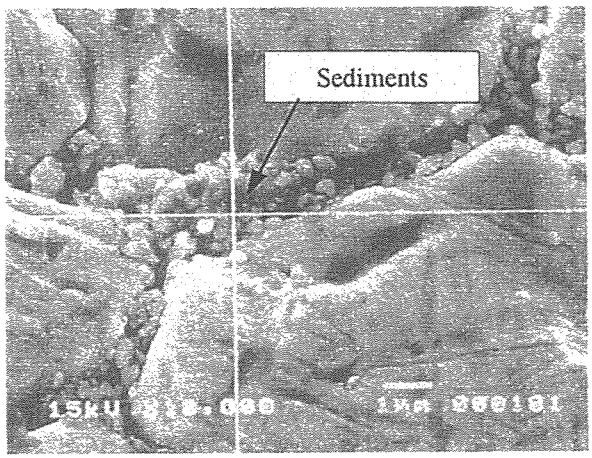

Fig.11 Scanning Electron (SE) image of crack area (TP41)

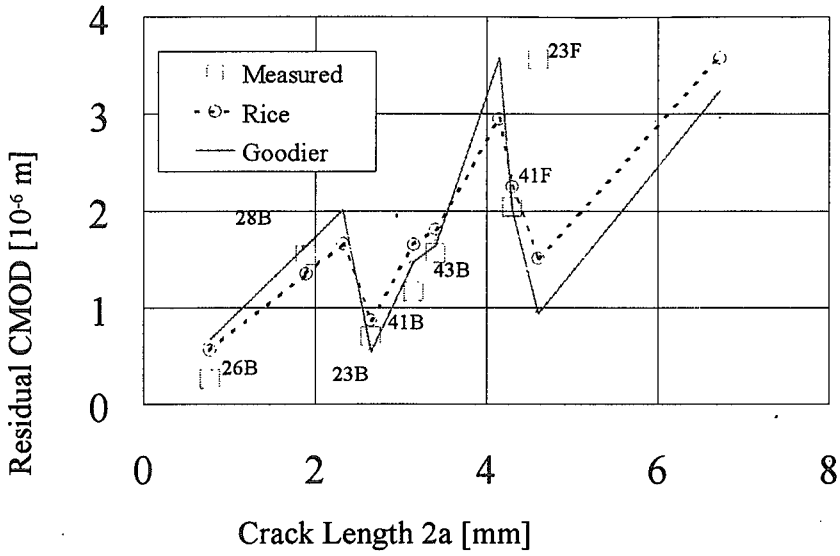

Fig.12 Comparison of CMOD measured and analyzed values

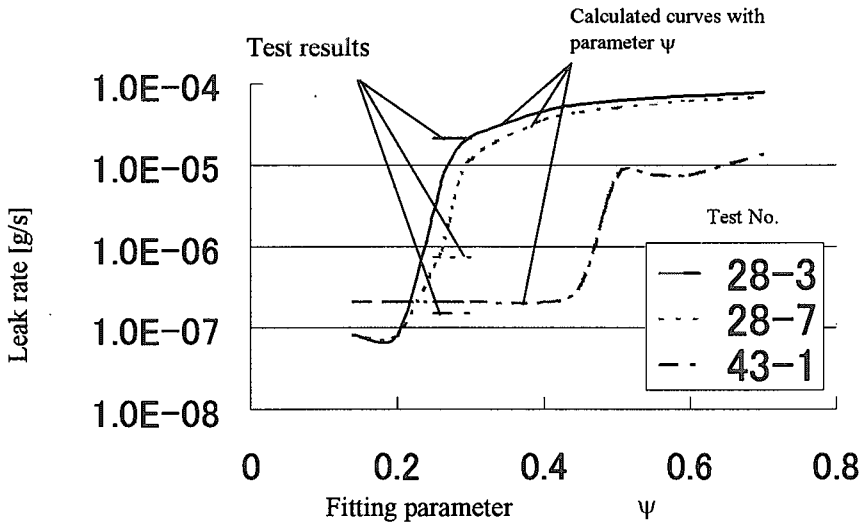

Fig.13 Relation of leak rate and fitting parameter ψ

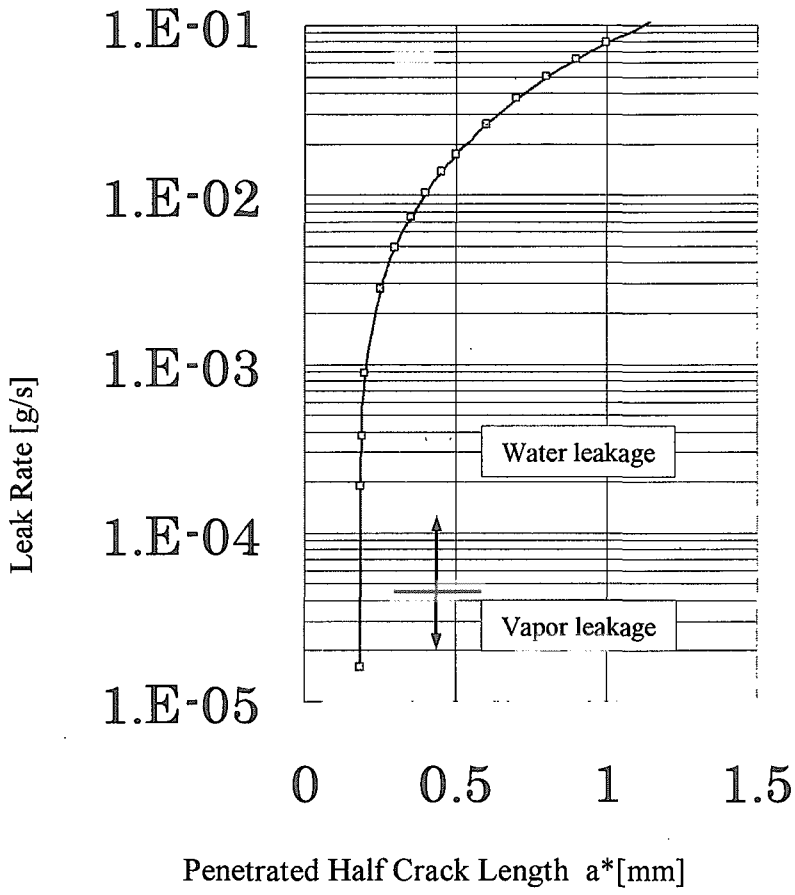

Fig.14 Evaluation of leak rate under present ITER design condition

国際単位系 (SI) と換算表

表 1　SI基本単位および補助単位

量	名称	記号
長さ	メートル	m
質量	キログラム	kg
時間	秒	s
電流	アンペア	A
熱力学温度	ケルビン	K
物質量	モル	mol
光度	カンデラ	cd
平面角	ラジアン	rad
立体角	ステラジアン	sr

表 2　SIと併用される単位

名称	記号
分，時，日	min，h，d
度，分，秒	°，′，″
リットル	l，L
トン	t
電子ボルト	eV
原子質量単位	u

1 eV = 1.60218 × 10^{-19} J

1 u = 1.66054 × 10^{-27} kg

表 3　固有の名称をもつSI組立単位

量	名称	記号	他のSI単位による表現
周波数	ヘルツ	Hz	s^{-1}
力	ニュートン	N	$m \cdot kg/s^2$
圧力，応力	パスカル	Pa	N/m^2
エネルギー，仕事，熱量	ジュール	J	N·m
工率，放射束	ワット	W	J/s
電気量，電荷	クーロン	C	A·s
電位，電圧，起電力	ボルト	V	W/A
静電容量	ファラド	F	C/V
電気抵抗	オーム	Ω	V/A
コンダクタンス	ジーメンス	S	A/V
磁束	ウェーバ	Wb	V·s
磁束密度	テスラ	T	Wb/m^2
インダクタンス	ヘンリー	H	Wb/A
セルシウス温度	セルシウス度	℃	
光束	ルーメン	lm	cd·sr
照度	ルクス	lx	lm/m^2
放射能	ベクレル	Bq	s^{-1}
吸収線量	グレイ	Gy	J/kg
線量当量	シーベルト	Sv	J/kg

表 4　SIと共に暫定的に維持される単位

名称	記号
オングストローム	Å
バーン	b
バール	bar
ガル	Gal
キュリー	Ci
レントゲン	R
ラド	rad
レム	rem

1 Å = 0.1 nm = 10^{-10} m

1 b = 100 fm^2 = 10^{-28} m^2

1 bar = 0.1 MPa = 10^5 Pa

1 Gal = 1 cm/s^2 = 10^{-2} m/s^2

1 Ci = 3.7 × 10^{10} Bq

1 R = 2.58 × 10^{-4} C/kg

1 rad = 1 cGy = 10^{-2} Gy

1 rem = 1 cSv = 10^{-2} Sv

表 5　SI接頭語

倍数	接頭語	記号
10^{18}	エクサ	E
10^{15}	ペタ	P
10^{12}	テラ	T
10^{9}	ギガ	G
10^{6}	メガ	M
10^{3}	キロ	k
10^{2}	ヘクト	h
10^{1}	デカ	da
10^{-1}	デシ	d
10^{-2}	センチ	c
10^{-3}	ミリ	m
10^{-6}	マイクロ	μ
10^{-9}	ナノ	n
10^{-12}	ピコ	p
10^{-15}	フェムト	f
10^{-18}	アト	a

（注）

1. 表1－5は「国際単位系」第5版，国際度量衡局 1985年刊行による。ただし，1 eVおよび1 uの値はCODATAの1986年推奨値によった。
2. 表4には海里，ノット，アール，ヘクタールも含まれているが日常の単位なのでここでは省略した。
3. barは，JISでは流体の圧力を表わす場合に限り表2のカテゴリーに分類されている。
4. EC閣僚理事会指令ではbar，barnおよび「血圧の単位」mmHgを表2のカテゴリーに入れている。

換算表

力	N(=10^5 dyn)	kgf	lbf
	1	0.101972	0.224809
	9.80665	1	2.20462
	4.44822	0.453592	1

粘度　1 Pa·s(N·s/m^2) = 10 P(ポアズ)(g/(cm·s))

動粘度　1 m^2/s = 10^4 St(ストークス)(cm^2/s)

圧力	MPa(=10 bar)	kgf/cm^2	atm	mmHg(Torr)	lbf/in^2(psi)
	1	10.1972	9.86923	7.50062×10^3	145.038
	0.0980665	1	0.967841	735.559	14.2233
	0.101325	1.03323	1	760	14.6959
	1.33322×10^{-4}	1.35951×10^{-3}	1.31579×10^{-3}	1	1.93368×10^{-2}
	6.89476×10^{-3}	7.03070×10^{-2}	6.80460×10^{-2}	51.7149	1

エネルギー・仕事・熱量	J(=10^7 erg)	kgf·m	kW·h	cal(計量法)	Btu	ft·lbf	eV
	1	0.101972	2.77778×10^{-7}	0.238889	9.47813×10^{-4}	0.737562	6.24150×10^{18}
	9.80665	1	2.72407×10^{-6}	2.34270	9.29487×10^{-3}	7.23301	6.12082×10^{19}
	3.6×10^6	3.67098×10^5	1	8.59999×10^5	3412.13	2.65522×10^6	2.24694×10^{25}
	4.18605	0.426858	1.16279×10^{-6}	1	3.96759×10^{-3}	3.08747	2.61272×10^{19}
	1055.06	107.586	2.93072×10^{-4}	252.042	1	778.172	6.58515×10^{21}
	1.35582	0.138255	3.76616×10^{-7}	0.323890	1.28506×10^{-3}	1	8.46233×10^{18}
	1.60218×10^{-19}	1.63377×10^{-20}	4.45050×10^{-26}	3.82743×10^{-20}	1.51857×10^{-22}	1.18171×10^{-19}	1

1 cal = 4.18605 J(計量法)

= 4.184 J　(熱化学)

= 4.1855 J　(15 °C)

= 4.1868 J(国際蒸気表)

仕事率　1 PS(仏馬力)

= 75 kgf·m/s

= 735.499 W

放射能	Bq	Ci
	1	2.70270×10^{-11}
	3.7×10^{10}	1

吸収線量	Gy	rad
	1	100
	0.01	1

照射線量	C/kg	R
	1	3876
	2.58×10^{-4}	1

線量当量	Sv	rem
	1	100
	0.01	1

（86年12月26日現在）

Applicability of LBB Concept to Tokamak-type Fusion Machine